The stellar kinematics and populations of boxy bulges: cylindrical rotation and vertical gradients[*]

Michael J. Williams,[1,2]† Michel A. Zamojski,[3] Martin Bureau,[1] Harald Kuntschner,[2] Michael R. Merrifield,[4] P. Tim de Zeeuw[2,5] and Konrad Kuijken[5]

[1]*Sub-Department of Astrophysics, University of Oxford, Denys Wilkinson Building, Keble Road, Oxford OX1 3RH*
[2]*European Southern Observatory, Karl-Schwarzschild-Str. 2, D-85748 Garching bei München, Germany*
[3]*Spitzer Science Center, California Institute of Technology, Pasadena, CA 91125, USA*
[4]*School of Physics and Astronomy, University of Nottingham, Nottingham NG7 2RD*
[5] *Sterrewacht Leiden, Universiteit Leiden, Postbus 9513, 2300 RA Leiden, the Netherlands*

ABSTRACT

Boxy and peanut-shaped bulges are seen in about half of edge-on disc galaxies. Comparisons of the photometry and major-axis gas and stellar kinematics of these bulges to simulations of bar formation and evolution indicate that they are bars viewed in projection. If the properties of boxy bulges can be entirely explained by assuming that they are bars, then this may imply that their hosts are pure disc galaxies with no classical bulge. A handful of these bulges, including that of the Milky Way, have been observed to rotate cylindrically, i.e. with a mean stellar velocity independent of height above the disc. In order to assess whether such behaviour is ubiquitous in boxy bulges, and whether a pure disc interpretation is consistent with their stellar populations, we have analysed the stellar kinematics and populations of the boxy or peanut-shaped bulges in a sample of five edge-on galaxies. We placed slits along the major axis of each galaxy and at three offset but parallel positions to build up spatial coverage. The boxy bulge of NGC 3390 rotates perfectly cylindrically within the spatial extent and uncertainties of the data. This is consistent with the metallicity and α-element enhancement of the bulge, which are the same as in the disc. This galaxy is thus a pure disc galaxy. The boxy bulge of ESO 311−G012 also rotates very close to cylindrically. The boxy bulge of NGC 1381 is neither clearly cylindrically nor non-cylindrically rotating, but it has a negative vertical metallicity gradient and is α-enhanced with respect to its disc, suggesting a composite bulge comprised of a classical bulge and bar (and possibly a discy pseudo-bulge). The rotation of the peanut-shaped bulge of NGC 5746 is difficult to classify, but the peanut-shaped bulge of IC 4767 does not rotate cylindrically. Thus, even this relatively small sample is sufficient to demonstrate that boxy bulges display a range of rotational and population properties, indicating that they do not form a homogeneous class of object.

Key words: galaxies: abundances – galaxies: bulges – galaxies: kinematics and dynamics – galaxies: stellar content.

1 INTRODUCTION

The central regions of disc galaxies host bulges whose nature (or absence) must be explained by any model of galaxy formation and evolution. A bulge is a physical protrusion of stars above and below the plane of the disc and/or an excess of light above the inward extrapolation of the radial exponential profile of the disc. There are three principal observational classes of bulges: classical bulges, pseudo-bulges, and boxy or peanut-shaped bulges (see e.g. Athanassoula 2005).

Classical bulges have dynamical and photometric properties and stellar populations that are similar to elliptical galaxies of the same mass (Kormendy & Illingworth 1982; Davies et al. 1983; Emsellem et al. 2004; Kormendy & Kennicutt 2004; Falcón-Barroso et al. 2006; Thomas & Davies 2006; MacArthur, González & Courteau 2009) and are thought to be the end products of the same formation

processes: either monolithic collapse (e.g. Eggen, Lynden-Bell & Sandage 1962; Larson 1974; Carlberg 1984; Pipino & Matteucci 2004) or multiple hierarchical mergers (e.g. White & Rees 1978; Cole et al. 1994; Thomas, Greggio & Bender 1999).

Pseudo-bulges have embedded spiral structure, disc-like near-exponential light profiles, flattened axial ratios and rotation-dominated dynamics (see Kormendy & Kennicutt 2004, and references therein). They are thought to be secularly rearranged disc material that was driven inwards by bars, ovals and possibly spiral arms. The observational constraints on the stellar populations of pseudo-bulges are less strong because studies have focused on bigger and brighter classical bulges, decomposing their extended star formation history is more complicated than in classical bulges and ellipticals, and dust is a significant problem for the late-type discs in which pseudo-bulges are more usually found. Nevertheless, the available population data are not strongly inconsistent with the secular model (Peletier et al. 1999; Gadotti & dos Anjos 2001, but see the pilot sample of MacArthur et al. 2009).

An important third class of bulge, and the focus of this paper, is the boxy and peanut-shaped bulges, which are present in about half of edge-on disc galaxies (Lütticke, Dettmar & Pohlen 2000). Their major-axis stellar and gas kinematics (Kuijken & Merrifield 1995; Bureau & Freeman 1999; Merrifield & Kuijken 1999; Chung & Bureau 2004; Méndez-Abreu et al. 2008) and light profiles (Bureau et al. 2006) are consistent with simulations of the formation and buckling of galactic bars (Combes et al. 1990; Raha et al. 1991; Athanassoula & Bureau 1999; Bureau & Athanassoula 2005) and point to them being bars viewed in projection. Peanut-shaped bulges are thought to be bars whose orientation is exactly perpendicular to the line of sight, while boxy bulges are seen in galaxies whose bar is at an intermediate angle. Bars oriented exactly parallel to the line of sight do not appear boxy or peanut shaped. In that sense, boxy and peanut-shaped bulges are not the axisymmetric features normally thought of as 'bulges'. Since the dominant model is that they are bars, which are not the end products of collapse or merger, but rather redistributed disc material, boxy bulges are also sometimes referred to as pseudo-bulges. However, for the purposes of clarity in this paper, we avoid this, since boxy bulges are truly thick.

In the absence of transformational mergers, bars, which are found in two-thirds of disc galaxies (Eskridge et al. 2000; Whyte et al. 2002; Marinova & Jogee 2007), are expected to play a crucial and perhaps dominant role in disc galaxy evolution (e.g. Sellwood & Wilkinson 1993; Kormendy & Kennicutt 2004; Hopkins et al. 2010). Boxy and peanut-shaped bulges therefore provide a unique perspective on a feature that is crucial for understanding galaxy evolution. By observing them above the plane of the disc, one can determine the intrinsic properties of bars in a way that is almost free of thin disc light pollution. Moreover, the observed dynamics of bars as a function of height above the plane is a crucial additional constraint on models of the nature of bulges, including ruling out the presence of a dynamically hot classical bulge/merger remnant. For example, Shen et al. (2010) modelled the line-of-sight mean velocity and velocity dispersion of M giant stars observed by the BRAVA survey in the Milky Way bulge (Howard et al. 2009). They placed an extremely low upper limit on the mass of any hot spheroid component, $\lesssim 7$ per cent; i.e. the Milky Way appears to be a pure disc galaxy (but see Babusiaux et al. 2010). Giant pure disc galaxies present an acute challenge for cosmological simulations of galaxy formation (e.g. van den Bosch 2001; Carollo et al. 2007; Dutton 2009; Kormendy et al. 2010).

Perhaps the most unusual property of dynamical models of bars viewed in projection is that, within the bulge, the rotational velocity does not change with height (e.g. Combes et al. 1990; Athanassoula & Misiriotis 2002). That is to say, lines of constant velocity are parallel to each other and perpendicular to the major axis, such that $\partial v/\partial|z| \sim 0$, where v is the line-of-sight velocity and z is along the minor axis of the (edge-on) galaxy. This unusual behaviour was first observed in the boxy bulge of NGC 4565 by Kormendy & Illingworth (1982), who named it 'cylindrical rotation'. It has since been noted in the following eight galaxies, all of which have a bulge that is, more or less, boxy: NGC 128 (Jarvis 1990), NGC 3069 (Shaw, Wilkinson & Carter 1993), NGC 1055 (Shaw 1993), NGC 4442 (Bettoni & Galletta 1994), NGC 7332 (Fisher, Illingworth & Franx 1994; Falcón-Barroso et al. 2004), NGC 4220 and 4425 (Falcón-Barroso et al. 2006), and the Milky Way (Howard et al. 2009). In simulations, all bulges that rotate cylindrically are boxy or peanut shaped, but not all boxy or peanut-shaped bulges rotate cylindrically (Athanassoula & Misiriotis 2002). Cylindrical rotation is not present (or has not been reported) in simulated unbarred galaxies, or in observations of classical bulges, where rotational velocity falls systematically with height within the bulge (see Fig. 1 for two illustrative examples from the SAURON sample; de Zeeuw et al. 2002; Emsellem et al. 2004).

In our search of the literature, we found no observations of the absence of cylindrical rotation in a boxy bulge. One of the goals of the present targeted study of boxy bulges is to determine whether this is confirmation bias or whether cylindrical rotation is truly ubiquitous in boxy bulges and therefore a requisite property of all realistic models of bars. The extent or absence of cylindrical rotation in boxy bulges would be of interest because it might constrain the concentration of the dark haloes (Athanassoula & Misiriotis 2002).

Our second goal is to examine the stellar populations of boxy bulges. The null hypothesis might be that, since bars are secularly rearranged disc material (rather than material accreted or formed during rapid mergers), the metallicities of boxy bulges should be similar to those of their host discs. If, however, the metallicities of boxy bulges differ from those of their discs, or if they have metallicity gradients, this is not necessarily a problem for the bar buckling scenario. As pointed out by Freeman (2008), the stars that have been scattered furthest from the disc are the oldest stars and therefore formed from the least metal-enriched fuel. The buckling process may therefore establish a negative minor-axis metallicity gradient. Indeed, such behaviour is observed in the Milky Way (Zoccali et al. 2008) and in NGC 4565, the archetypal boxy, cylindrically rotating bulge (Proctor, Sansom & Reid 2000). The strength of the metallicity gradient established in this way must be a function of both the rate of enrichment in the disc and the time-scale over which the bar buckles and heats the disc. The process must also establish a corresponding positive age gradient. We know of no chemodynamical simulations of this process and, in particular, no prediction of the extent to which minor-axis gradients in boxy bulges are expected to differ from those in classical bulges.

Moreover, we know of no prediction regarding the relative abundance of α-elements in boxy bulges. The naive expectation, however, is that the [α/Fe] ratio of a boxy bulge should match that of its host disc. It is difficult to understand how secularly rearranged disc material could be segregated such that a boxy bulge of disc origin is α-enhanced with respect to its disc. Enhanced [α/Fe] ratios indicate that material was α-enriched by core-collapse (Type II) supernovae before Type Ia supernovae Fe enrichment, which implies a formation time-scale of $\lesssim 1$ Gyr. Bulges that are α-enhanced with respect to their disc therefore contain stars formed on much shorter time-scales than the disc stars (and not just at earlier times). If observed in a galaxy, this would suggest that its bulge is at least partially
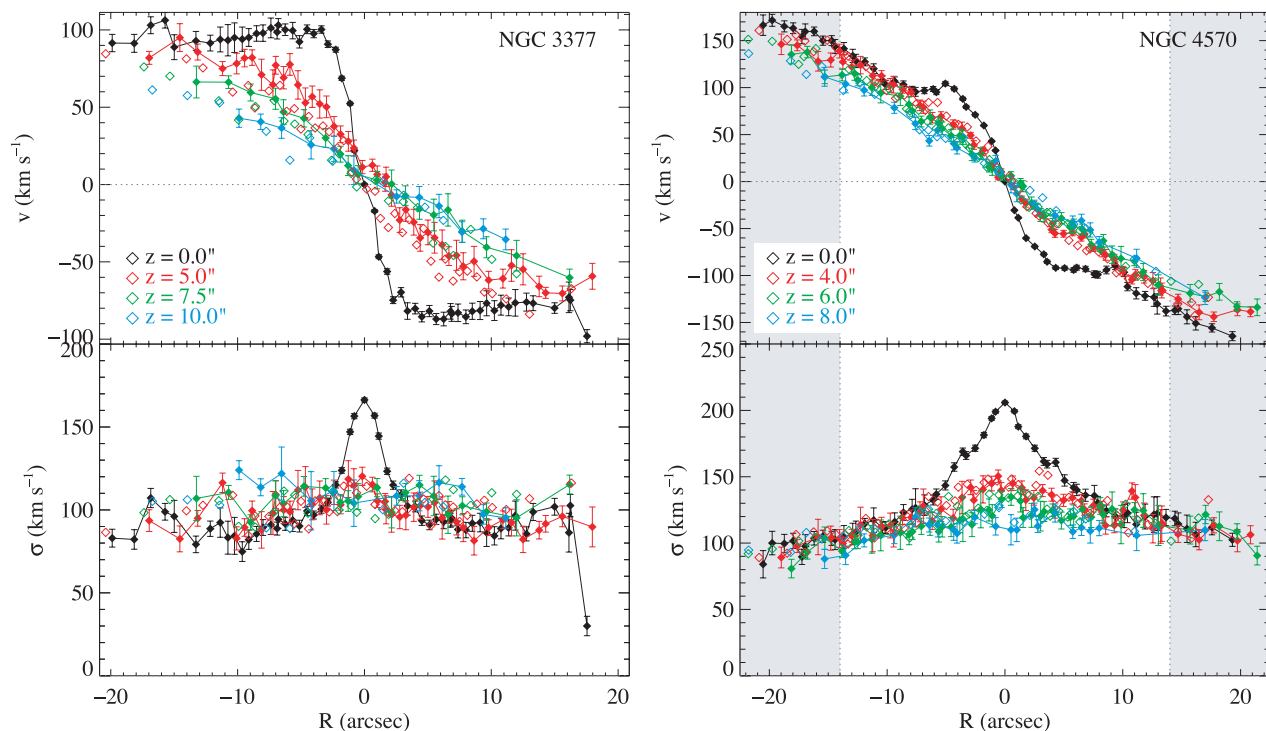
Figure 1. Stellar line-of-sight rotation curves and velocity dispersion profiles for two non-cylindrically rotating edge-on galaxies from the SAURON sample (the fast rotator elliptical NGC 3377 and the classical bulge of the S0 NGC 4570), constructed by extracting pseudo-slits from the integral-field kinematics presented in Emsellem et al. (2004). The stellar kinematics along the major axis are shown in black, and those from pseudo-slits offset from, but parallel to, the major axis are shown in order of increasing distance from the major axis in red, green and blue. The offset distance z is shown. Data from one side of the major axis are shown as filled diamonds (joined by lines) and data from the other side as open diamonds (with error bars omitted for clarity). The vertical dotted lines at $R = 14$ arcsec for NGC 4570 indicate the effective radius R_e, i.e. the approximate extent of the bulge (beyond which the figure is shaded grey). The effective radius of NGC 3377 is 38 arcsec, i.e. beyond the radial range shown. Note that, within each bulge at a given R, v falls systematically with height above the major axis, i.e. the rotation pattern is not cylindrical.

comprised of material formed in a merger or rapid collapse, or material of external origin. We discuss some of the issues that complicate this naive expectation in Section 5.

In this paper, we present a focused spectroscopic analysis of the boxy bulges of five edge-on disc galaxies. In Section 2 we describe the sample, the data and their reduction. We present the derived stellar kinematics in Section 3 and the stellar populations in Section 4. We summarize our results and suggest future work in Section 5.

2 OBSERVATIONS AND DATA REDUCTION

Our sample consists of five galaxies whose bulges were classified as boxy or peanut shaped by Lütticke et al. (2000) using Digitized Sky Survey images and whose major-axis stellar/gas kinematics and stellar structure have been homogeneously studied (Bureau & Freeman 1999; Chung & Bureau 2004; Bureau et al. 2006). All of the galaxies are edge-on or nearly edge-on. NGC 5746 is the furthest from edge-on in the sample. It is inclined at 85°5, measured by fitting an ellipse to the prominent ring visible in near-infrared *Spitzer* Infrared Array Camera images (PI: Giovanni Fazio).

We observed the sample using the New Technology Telescope's ESO Multi-Mode Instrument (EMMI) in long-slit spectroscopy mode. The observations were made in 2000 January, May and October (programmes 64.N-0545, 65.N-0126 and 66.B-0073, respectively). We positioned the slit along the major axis and then parallel to it at three offset positions. In this way we built up spa-

tial coverage similar to that of a sparse, wide-field integral-field spectrograph. We present the sample properties and slit positions in Table 1. We show the slits superimposed on images of the sample in Fig. 2.

We observed three other galaxy bulges (NGC 1055, 1247 and 7123), two of which are not boxy, during the runs but we dropped them from the present analysis because the data are poor or incomplete, and the SAURON project and other work have superseded any contribution these observations could have made to our understanding of the dynamics and populations of classical bulges (e.g. Proctor & Sansom 2002; Emsellem et al. 2004; Falcón-Barroso et al. 2006; Thomas & Davies 2006).

We reduced the data using standard techniques in Image Reduction and Analysis Facility (IRAF), yielding flat-fielded, wavelength-calibrated sky-subtracted two-dimensional spectra at four slit positions for each galaxy. Exposure times ranged from 30 min for the major-axis slits to up to 3 h for the slits furthest from the disc. The reduced two-dimensional spectra were linearly binned in wavelength and covered the range of 4830–5470 Å. The spectral resolution of the spectra is 1.0 Å full width at half-maximum (equivalent to $\sigma_{inst} \approx 25$ km s^{-1} at 5150 Å). The spatial axis has a pixel scale of 0.9 arcsec pixel^{-1}. We determined the central bin (i.e. the spectrum for which the cylindrical radius $R = 0$) using a Sérsic fit to the profile of each spectrum. This measurement is correct at the sub-arcsec level for the major-axis slit, but is uncertain by $\lesssim 5$ arcsec away from the mid-plane, where the radial profile is noisy and weakly peaked. The central bin for each slit may therefore be a point that does not lie exactly on the minor axis. This uncertainty may introduce a small,

Table 1. Sample properties and slit positions.

Galaxy	RC3 classification	Bulge type	Bulge extent (arcsec)	Offset slit positions (arcsec)		
ESO 311–G012	S0/a?	Boxy	15	6.0	9.0	12
IC 4767	S0+ˆ	Peanut	18	3.5	5.25	7
NGC 1381	SA0	Boxy	10	6.0	9.0	12
NGC 3390	Sb	Boxy	10	5.0	7.5	10
NGC 5746	SAB(rs)b?	Peanut	20	13.5	20.25	27

Note. Bulge extent is defined here as the radius of the maximum scaleheight of the disc, as measured from the vertical photometric parametrizations presented in Bureau et al. (in preparation). The offset slit positions are the distance each slit was offset from the major axis of the galaxy.
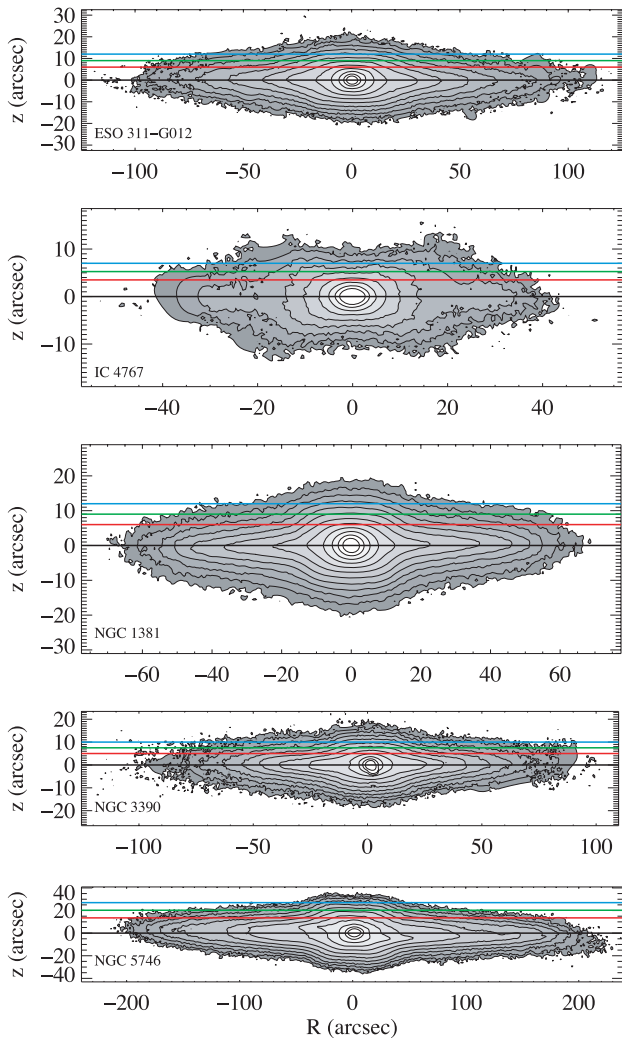

Figure 2. *K*-band images of the sample galaxies with the slits overlaid. Contours are separated by 0.5 mag. Images are taken from Bureau et al. (2006).

systematic relative offset between the kinematic profiles derived for each slit.

Spectrophotometric flux standards were not observed during the observing runs, so we are unable to precisely flux calibrate our data. However, as described in Section 4, this does not significantly affect our ability to measure line strengths.

3 STELLAR KINEMATICS

3.1 Methods

In order to determine the stellar kinematics, we first binned the data spatially to enhance the signal-to-noise ratio (S/N). To measure the line-of-sight mean velocity v, we typically binned to an S/N of about 10 per Å, but lowered this to 5 per Å for a few of the most offset slits. The outermost bin in each slit often does not reach the desired S/N level, but we analysed it (and included in these figures) for completeness. To measure the velocity dispersion σ, we rebinned the data to twice the S/N, sacrificing spatial resolution.

We extracted absorption-line stellar kinematics from the binned spectra using penalized pixel fitting (PPXF; Cappellari & Emsellem 2004). All galaxies except NGC 1381 show clear signs of Hβ or [O III] emission in their major-axis spectrum, but the data in each bin are of insufficient S/N to constrain the emission-line properties and subtract the emission in a physically motivated way using, for example, GANDALF (Sarzi et al. 2006). To derive the absorption-line stellar kinematics, the appropriate spectral regions are therefore simply masked.[1] We also masked a series of bad columns on the CCD at a rest wavelength of ≈5050 Å.

We used a subset of 88 stars from the MILES library of 985 observed stellar spectra as templates (Sánchez-Blázquez et al. 2006). The MILES spectra have a spectral resolution of 2.3 Å while our spectra have a resolution of 1.0 Å, so we first degraded our spectra to the MILES resolution. In principle, the penalized pixel fitting algorithm can robustly recover dispersions down to around half of this degraded spectral resolution, i.e. ≈28 km s^{-1}. Using the Fourier correlation quotient method (Bender 1990) and a template star with a spectral resolution of ≈32 km s^{-1}, Chung & Bureau (2004) measured dispersions of >50 km s^{-1} along the major axis of all five galaxies in the present sample. Since the true dispersions of these galaxies are of the order of the spectral resolution of the MILES library, working at the MILES spectral resolution should not affect our results for the line-of-sight velocity dispersion. To verify this, we repeated the kinematic extraction for NGC 1381 working at the spectral resolution of our observations. To do this, we used degraded template spectra from the ELODIE library of 1388 stars (whose spectra have a resolution of 12 km s^{-1}, i.e. higher than that of our observations; Prugniel & Soubiran 2001). Within the uncertainties, the v and σ radial profiles we obtained agree with those recovered using the MILES library, with no sign of any systematic disagreement.

---

[1] Note that we do treat emission properly when determining the absorption-line strengths in Section 4, where we bin to a much higher S/N.

Our data are of insufficient S/N to constrain h_3 (skewness) and h_4 (kurtosis) using a Gauss–Hermite parametrization of the line-of-sight velocity distribution (LOSVD). We therefore enforce a pure Gaussian LOSVD. Our conclusions regarding cylindrical rotation, which depend only on v, are not affected by this decision.

We estimated the uncertainties on the derived kinematics by running pPXF on 100 random realizations of each spectrum. The realizations were constructed by adding wavelength-independent Gaussian noise assuming Poisson statistics. To these uncertainties we added uncertainties due to wavelength calibration, which we estimate to be $\lesssim 0.2$ Å, i.e. $\lesssim 10\,\mathrm{km\,s^{-1}}$. These wavelength calibration uncertainties generally dominate the uncertainties in v, but are less important for σ, where the spectral noise dominates.

3.2 Results

The line-of-sight mean stellar velocity v and velocity dispersion σ calculated as described above are presented in Fig. 3. The kinematics of the major-axis slit are shown in black and those of the offset slits are shown in order of increasing distance from the major axis in red, green and blue. In each plot, we indicate the approximate extent of the bulge with dotted vertical lines.

The boxy bulge of NGC 3390 is a clear example of cylindrical rotation. Within the uncertainties, it shows no systematic variation of rotational velocity as a function of height at all.

The behaviour of the boxy bulge of ESO 311–G012 is close to cylindrical. The major-axis rotation is somewhat discrepant from that of the offset slits; the rotation curve along the plane of the disc is 'double-humped', while those of the offset slits are not. This does not mean that the boxy bulge is not rotating cylindrically. The strong double-hump feature is seen in simulations of barred galaxies (e.g. Bureau & Athanassoula 2005) and is likely the dynamical signature of bar-driven inward transport of material (e.g. Kormendy & Kennicutt 2004), which leads to the formation of a flattened round central excess of material, i.e. a pseudo-bulge. The distinguishing feature of cylindrical rotation is therefore that v does not vary systematically with height away from the major axis, which is true of ESO 311–G012. Taken together, we interpret the presence of a double hump in the rotation curve along the major axis and cylindrical rotation in the offset slits as consistent with simulations of the formation and dynamics of bars (Combes et al. 1990; Athanassoula & Misiriotis 2002; Bureau & Athanassoula 2005).

The classification of the type of rotation in the boxy bulge of NGC 1381 is marginal. The velocity along the major axis is extremely discrepant from that along the offset slits. The slits at 6 and 9 arcsec are corotating, but the slit at 12 arcsec is of extremely low S/N and is binned to a correspondingly coarse spatial resolution. While this galaxy lacks the clear systematic decrease in v with increasing z seen in the examples in Fig. 1, it is not a clean case of cylindrical rotation either.

The same is true of the peanut-shaped bulge of NGC 5746, but the picture is further complicated here by the rather irregular rotation curves within the bulge. This may be due to the prominent dust 'lane' in NGC 5746, which, because this galaxy is a few degrees away from edge-on, obscures a fraction of the galaxy. Strong absorption may cause the local mean line-of-sight velocity to differ significantly from the azimuthal velocity at the tangent point along the line of sight, and the extent of this difference may vary in a complicated way with distance along the minor axis.

The peanut-shaped bulge of IC 4767 is not cylindrically rotating. At negative R, even accounting for the uncertainties and the irregu-

larity of the rotation curve, v falls systematically with z. At positive R, the signature of non-cylindrical rotation is less clear.

Cylindrical rotation is therefore not a ubiquitous feature of boxy and peanut-shaped bulges. There is also some evidence that it is less strong or even absent in peanut-shaped bulges compared to boxy bulges. It is worth considering whether this might have a dynamical origin. In simulations, bars in edge-on galaxies appear peanut shaped when viewed with the bar perpendicular to the line of sight and boxy when the bar is at an intermediate angle (e.g. Combes et al. 1990). End-on bars appear neither boxy nor peanut shaped. The velocity fields of these simulated galaxies vary with the orientation of the bar in the sense that the closer the bar is to end-on (i.e. the less strongly peanut shaped it appears), the more closely packed are the lines of constant velocity (e.g. fig. 6 of Combes et al. 1990 and fig. 12 of Athanassoula & Misiriotis 2002). There is, however, no clear sign of a systemic strengthening or weakening of cylindrical rotation as the viewing angle varies in these published studies. Rather, the strength and extent of cylindrical rotation in the simulations of Athanassoula & Misiriotis (2002) are a function of dark halo concentration in the sense that less concentrated dark haloes host boxy bulges in which cylindrical rotation is absent or less extended.

On a different note, in ESO 311–G012, NGC 1381, 3390 and 5746 (i.e. all the galaxies with boxy or peanut-shaped bulges except IC 4767), there is a general downward trend in velocity dispersion with increasing height above the disc. This is most clear in ESO 311–G012 and NGC 5746. This behaviour is also seen in classical bulges (Fig. 1), but the details of the variation of the velocity dispersion with height were crucial constraints in the Milky Way models of Howard et al. (2009) and Shen et al. (2010). These authors placed an upper limit on the possible contribution of any dynamically hot spheroid component by comparing photometric and kinematic observations to dynamical models. Their analysis implies that the Milky Way has, at most, an extremely low-mass classical bulge, i.e. it is a pure disc galaxy (but see Babusiaux et al. 2010). Without a comparison to dynamical models custom-made for each galaxy, which is beyond the scope of this work, it is not possible here to draw such a strong conclusion on the basis of our velocity and dispersion profiles.

4 LINE STRENGTHS AND STELLAR POPULATIONS

4.1 Methods

The spatial variations of stellar population properties offer additional constraints on the nature and evolution of bulges. We therefore measured the strengths of the absorption lines present in our data (Hβ, Fe5015, Mg b, Fe5270, Fe5335 and Fe5406) in the Lick/IDS system (Burstein et al. 1984; Worthey 1994; Trager et al. 1998) and compared these to single stellar population (SSP) models, yielding SSP-equivalent luminosity-weighted ages, metallicities [Z/H] and α-element enhancement [α/Fe].

To make these measurements, we require a high S/N to reliably subtract nebular emission and thus accurately measure the absorption-line properties. We therefore binned the major-axis slit into three large bins: a single bin for the bulge and two disc bins (one from each side of the galaxy). We collapsed each of the three offset slits into a single bin dominated by bulge light (rejecting the very small amount of thick disc light at larger galactocentric radii). This yields one bulge-dominated measurement from the centre of the bulge, two disc-dominated measurements along the major axis and three minor-axis bulge measurements at increasing galactic height.
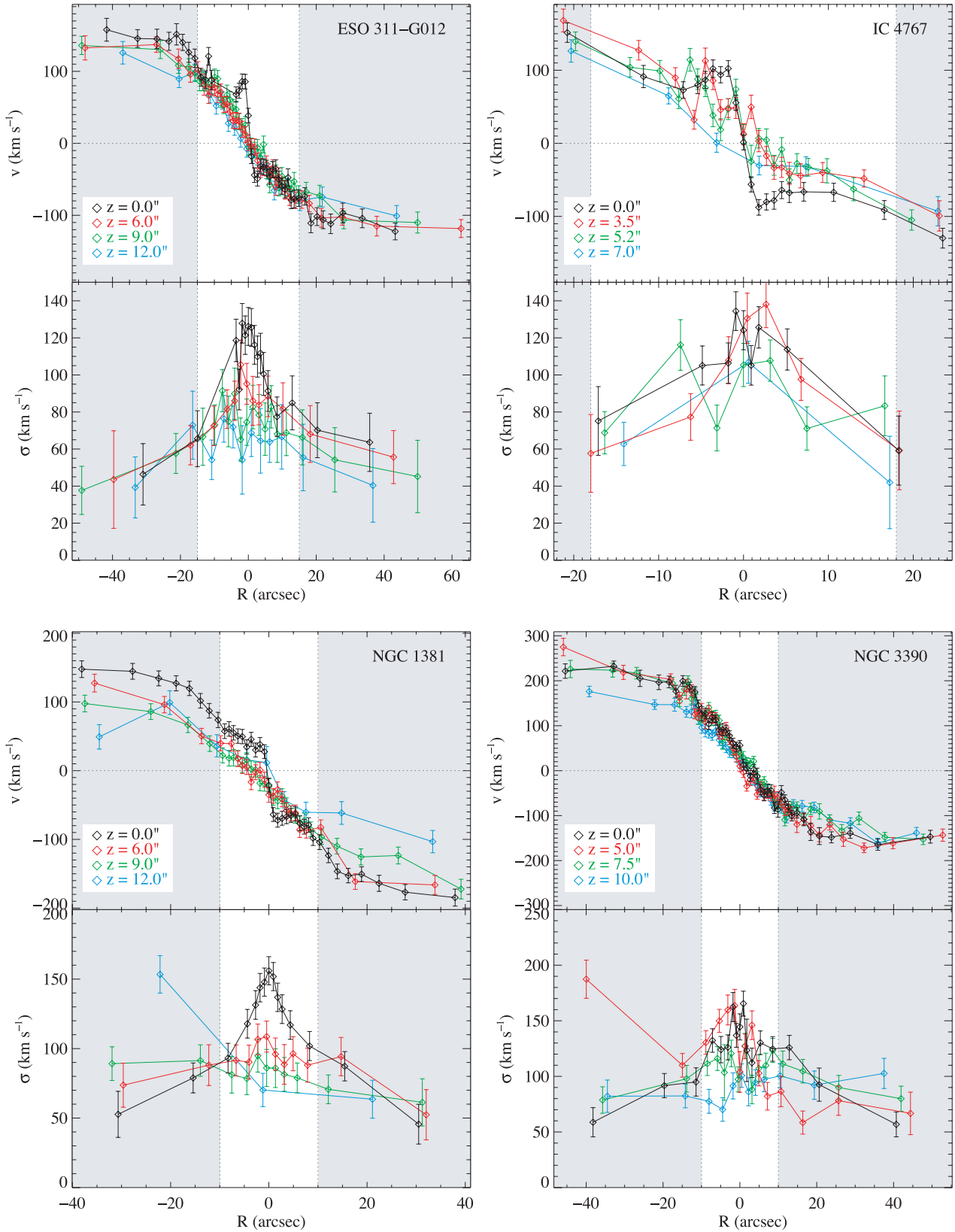
Figure 3. Stellar line-of-sight mean velocity (top) and velocity dispersion (bottom) for the five sample galaxies. The stellar kinematics of the major axis are shown in black, and those of the offset slits are shown in order of increasing distance from the major axis in red, green and blue. See Table 1 and Fig. 2 for the slit positions. The vertical dotted lines indicate the approximate extent of the bulge (see Table 1). The shaded regions at large radii therefore correspond roughly to the galaxy disc. The same systemic velocity has been subtracted from all points, determined from a pPXF fit to the total major axis spectrum.
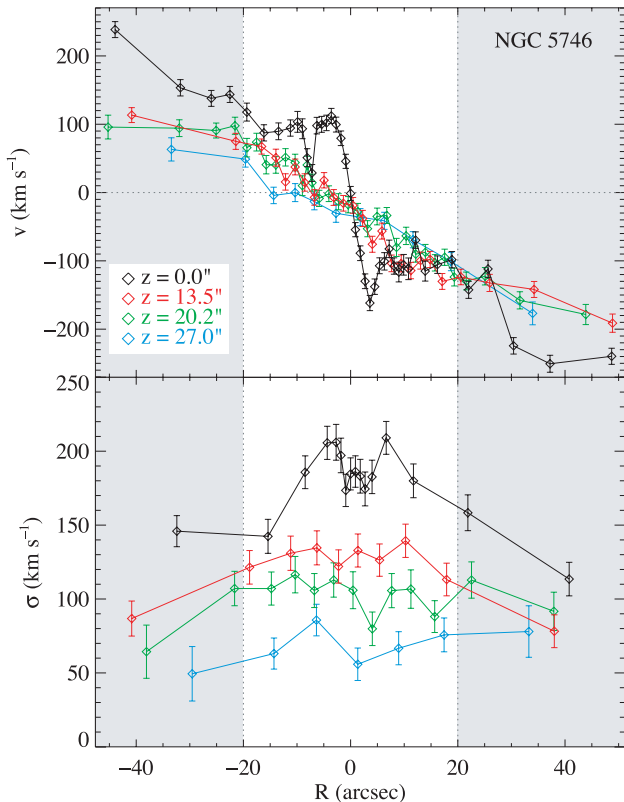
Figure 3 – *continued*

With data at four positions along the *z*-axis, it is not really possible to quantify vertical gradients (although as we discuss in Section 1, these are of interest). However, we can test our naive picture that a boxy bulge should have [α/Fe] similar to that of its host disc.

Of the absorption lines in our data, only Hβ provides a strong constraint on stellar age that is weakly dependent on metallicity (Worthey 1994), but this absorption feature is unfortunately often filled in by emission. To compare the population properties of galaxy discs and bulges, we therefore restrict our analysis to those galaxies whose major-axis disc spectra are either free of emission or of sufficient S/N to allow reliable subtraction of the Hβ emission using GANDALF (Sarzi et al. 2006). This is only true for NGC 1381, which has no emission, and NGC 3390. The analysis that follows is therefore restricted to these two galaxies only.

We show an example GANDALF fit in Fig. 4. The best-fitting GANDALF solution is comprised of the Hβ and [O III] emission lines and a combination of flux-calibrated MILES template stars that are convolved by an LOSVD and multiplied by a sixth-order polynomial to account for the relative continuum differences between our set-up and the MILES library. To produce an emission-cleaned spectrum that can be used to measure absorption-line properties and that can be compared to models, we subtract the GANDALF emission lines from the observed spectrum and divide them by the sixth-order polynomial, achieving a rough relative flux calibration. In practice, the polynomial is extremely slowly varying and close to first order over the bandpasses of the Lick indices, so this affects the measured line strengths at a level significantly below the uncertainties due to the noise.

It is then possible to measure the strengths of the lines in the Lick/IDS system, which we do using the method of Kuntschner (2000). But before these measurements are made, the spectra must be convolved with a wavelength-dependent Gaussian to account for the difference between the spectral resolution of our set-up and that of the Lick/IDS system. The resulting indices are further corrected for (1) the broadening effects of the galaxies' velocity dispersions (which generally reduce the strength of absorption features) and (2) the small systematic offsets caused by, for example, the remaining differences between the continuum shapes of our spectra and the Lick/IDS spectra. We apply the offsets from the MILES system given in the appendix of Paudel et al. (2010). This offset of course only affects the absolute value of the indices, not their spatial gradients.

We use the line strengths to measure stellar population properties using the models of Thomas, Maraston & Bender (2003). These models incorporate non-solar [α/Fe]. The best-fitting SSP-equivalent model for each spectrum is found by exploring an interpolated grid of model Lick indices in age, [Z/H] and [α/Fe]
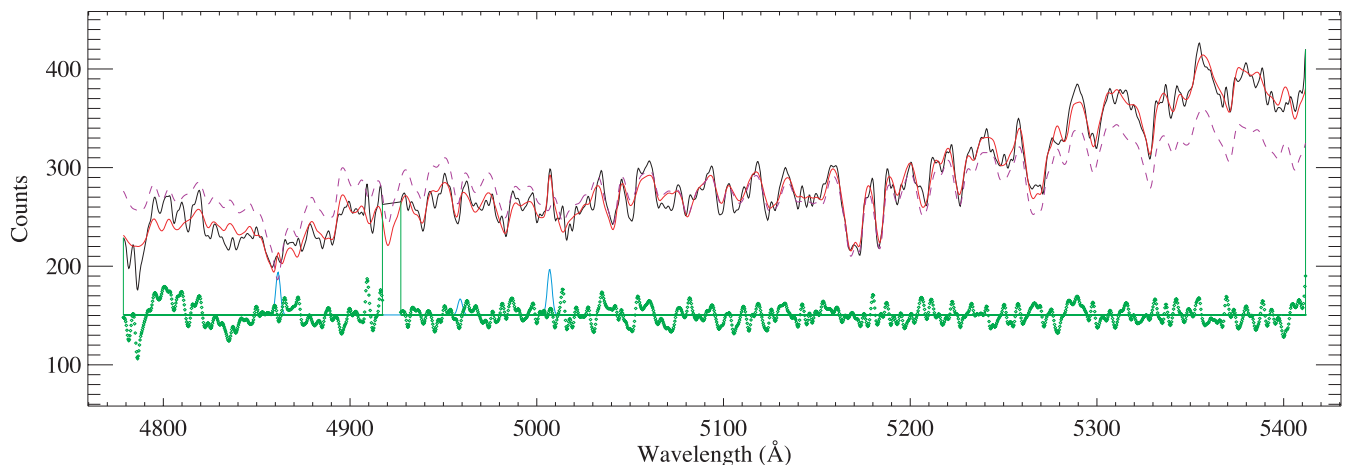

Figure 4. Example GANDALF fit for one of the two disc spectra of NGC 3390. We show the observed spectrum (degraded to the MILES resolution) in black and the GANDALF best fit in red. The green points are the difference between the best fit and the observed spectrum, shifted by an arbitrary positive offset so they appear on the scale. The best fit is comprised of the Hβ and [O III] emission lines (shown in blue) and a combination of MILES template stars that are convolved by an LOSVD (purple dashed line) and multiplied by a sixth-order polynomial to account for the relative continuum differences between our set-up and the MILES library. The anomalous feature at ≈4920 Å is due to a problem with the CCD and is masked for all analyses.

(see e.g. Proctor et al. 2000; Kuntschner et al. 2010). We exclude Fe5015 from this analysis. It is still sometimes contaminated by [O III] emission, it is close to the bad pixels on the CCD and it covers an extremely wide bandpass so is subject to relatively large continuum systematics and Lick offsets. This line provides very little additional constraints on the optimal SSP over those offered by the other three Fe lines.

4.2 Results

We show the derived Lick indices and corresponding SSP-equivalent luminosity-weighted age, [Z/H] and [α/Fe] as a function of height above the Galactic plane in Fig. 5. There are two additional points on the major axis ($z = 0$), which are the measurements from the two disc bins.

In both galaxies, there is no sign of a systematic trend in the age-sensitive Hβ line as a function of z or in the derived age.

In NGC 1381, there are broadly decreasing trends with increasing height in the metallicity-sensitive Fe and Mg lines. These are qualitatively similar to the minor-axis trends seen in the SAURON classical bulges shown in Fig. 1 [see Kuntschner et al. (2006) for the corresponding line strength maps]. The SSP-equivalent stellar population properties derived from these line strengths suggest that the bulge is comprised of an old stellar population, $\gtrsim 10$ Gyr with no systematic trend in age as a function of z, but there is a clear decreasing trend in [Z/H]. We also note that [α/Fe] in the bulge at large z is greater than that in the disc bins (and indeed the central bin of the major axis). The simplest interpretation of these results is that NGC 1381 is comprised of a disc and a bulge whose stars formed rapidly. This explains the general trend in [α/Fe] as a function of height, as disc light (with its lower [α/Fe]) contributes less and less to the integrated spectrum. In summary, the bulge of NGC 1381 is chemically similar to that of classical bulges and elliptical galaxies.

Given this classical bulge behaviour, how do we explain the boxy appearance of the bulge? We speculate that this is a composite bulge: its chemical properties are explained by the presence of a classical bulge, but its appearance suggests the simultaneous presence of a bar (which appears boxy in projection). This is consistent with the stellar rotation, neither cylindrical nor strongly non-cylindrical. The double hump of the rotation curve even hints at the presence of a small discy pseudo-bulge. This galaxy thus seems to have all three kinds of bulges.

The situation in NGC 3390 is much simpler. Within the (not insignificant) uncertainties, its bulge has no minor-axis metallicity gradient, and the [α/Fe] measurements in the bulge bins at large z are entirely consistent with those of the disc. That is to say, this galaxy's bulge is made of material similar to that in its disc, and the process that has scattered it to large z has not established a systematic metallicity gradient. This is consistent with the kinematics of this bulge, which is cylindrically rotating to great precision in all the slits (including the major axis). The simplest interpretation of NGC 3390 is therefore that it is a pure disc galaxy.

5 DISCUSSION

We analysed the kinematics and stellar populations of the boxy or peanut-shaped bulges of a sample of five edge-on disc galaxies. One boxy bulge (NGC 3990) rotates perfectly cylindrically, while another (ESO 311–G012) is very close to cylindrical. It is not possible to cleanly classify the rotation in the boxy bulge of NGC 1381 or the peanut-shaped bulge of NGC 5746. The strongly peanut-shaped
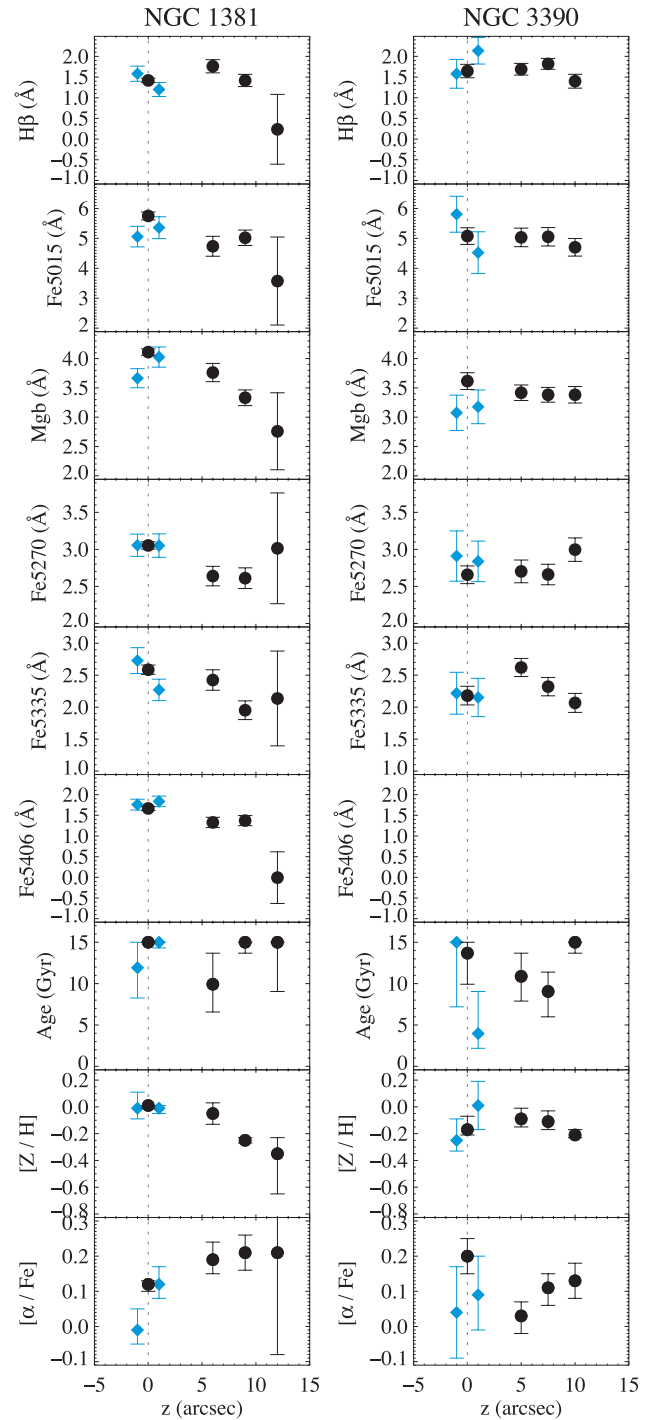

Figure 5. Lick indices and luminosity-weighted SSP-equivalent ages, metallicities and [α/Fe] ratios as a function of the perpendicular distance to the major axis for NGC 1381 and 3390. Measurements are made at the centre of the galaxy (black circle at $z = 0$), two disc bins along the major axis (blue diamonds) and three points at increasing distance along the minor axis (black circles at $z \neq 0$). The disc bins correspond to spectra at $z = 0$, but we added a spatial offset of ± 1 arcsec for clarity in these plots. The $z = 12$ arcsec bulge spectrum in NGC 1381 has some line strengths that are consistent with an equivalent width of zero, and the uncertainties in [α/Fe] for this bin extend over the full model grid. The position is shown merely for completeness. The Fe5406 feature is redshifted beyond the observed wavelength range for NGC 3390 and could therefore not be measured.

bulge of IC 4767 is in normal rotation, the velocity falling systematically with height. Cylindrical rotation is therefore not a ubiquitous behaviour in bulges that appear boxy or peanut shaped.

Our sample is small and this work is exploratory, but we also tentatively note that cylindrical rotation may be less strong or even absent in peanut-shaped bulges, compared to boxy bulges. While this is not a prediction of simulations, models are able to qualitatively reproduce a case like IC 4767 by reducing the central concentration of the dark halo (Athanassoula & Misiriotis 2002).

Low S/N and the presence of emission are less of a problem when determining absorption-line stellar kinematics than when measuring absorption-line strengths. We were therefore only able to measure minor-axis trends in Lick indices and derive luminosity-weighted SSP-equivalent age, [Z/H] and [α/Fe] for two of the five galaxies. Of these, NGC 3390 exhibits behaviour consistent with being a pure disc: there is no significant difference in [Z/H] and [α/Fe] between the disc and the boxy bulge at large galactic heights, suggesting that the boxy bulge formed from redistributed disc material. NGC 1381, however, shows a clear negative metallicity gradient as a function of z, while [α/Fe] in the bulge at large z is significantly enhanced compared to that in the disc. This behaviour is consistent with a simple disc + classical bulge model (e.g. Norris, Sharples & Kuntschner 2006, for the edge-on S0 NGC 3115). Combined with the marginal cylindrical rotation and the boxy shape of the bulge, this suggests that the centre of NGC 1381 hosts a composite bulge comprised of a classical bulge, a discy pseudo-bulge and a thick bar.

The naive expectation that we described in Section 1, that a boxy bulge should have the same [α/Fe] as its host disc if it formed through the bar buckling scenario and is part of a pure disc galaxy, is one part of our argument that NGC 3390 may be a pure disc galaxy. This picture is complicated by at least two issues as follows. (1) The disc could have formed rapidly and then buckled promptly, forming an α-enhanced thick bar, i.e. a boxy bulge, and (2) in a system made up of stars in which [α/Fe] is anticorrelated with [Z/H] (e.g. as seen in young stars in the Galaxy; Edvardsson et al. 1993), a negative spatial metallicity gradient would necessarily coincide with a positive spatial [α/Fe] gradient.

Regarding point (1), we note that the 'wild disc' scenario (in which early star formation in the progenitors of disc galaxies takes place on short time-scales in massive clumps; e.g. Noguchi 1999; Elmegreen, Elmegreen & Hirst 2004; Bournaud, Elmegreen & Elmegreen 2007) probably cannot explain how a bar could be α-enhanced with respect to its host disc. In dynamical simulations, these clumps rapidly migrate inwards through dynamical friction and combine to form an axisymmetric feature that would probably look like an α-enhanced classical bulge (in terms of both populations and dynamics). Chemodynamical simulations of bar formation are clearly necessary to clarify the issue.

Such studies should also address the more general questions raised by this work. (1) Is the double hump we see in the rotation curve along the major axis of two of the boxy and peanut-shaped bulges definitely associated with a flattened discy pseudo-bulge? How far does its influence extend above the plane? (2) How does the viewing angle of the bar affect the observed kinematics? For example, do we expect weaker cylindrical rotation in peanut-shaped bulges? This question was addressed by Athanassoula & Misiriotis (2002), but quantitative (rather than qualitative) comparisons to observations are necessary. (3) Do the minor-axis metallicity and age gradients of simulated bars differ systematically from those of classical bulges? (4) Can simulated bars form in a way that explains the presence of a positive minor-axis [α/Fe] gradient, as

seen in NGC 1381, without the additional presence of a classical bulge?

The α-enhanced bulge of NGC 1381 suggests that not all boxy bulges are found in pure disc galaxies (although some, including the Milky Way, may be). Since the prevalence of giant pure disc galaxies is an acute problem for simulations of galaxy formation in a cosmological context, it is clear that a combined analysis of the stellar dynamics and populations of the central regions of galaxies is an extremely powerful tool.

The sample we have studied in this work is unusual because it is dominated by boxy and peanut-shaped bulges. Such galaxies are unique laboratories to investigate the nature of the bars that drive secular evolution. Moreover, they raise the possibility that a demographically significant fraction of giant disc galaxies, making up about half the population, is composed of pure disc galaxies. We have shown that a property as simple as the degree of cylindrical rotation varies significantly among boxy/peanut-shaped bulges, as do the properties of their stellar populations. The driver of this variation is unknown, but may be a property as fundamental as dark halo concentration. Clearly, if we want to further our understanding of the formation of boxy and peanut-shaped bulges, we need data in larger quantities (to look for correlations with other galaxy properties such as environment and mass distribution) and at a higher S/N (to more accurately measure stellar population properties). Two-dimensional data from integral-field units would also be beneficial, allowing the dynamics to be modelled in detail.

REFERENCES

Athanassoula E., 2005, MNRAS, 358, 1477
Athanassoula E., Bureau M., 1999, ApJ, 522, 699
Athanassoula E., Misiriotis A., 2002, MNRAS, 330, 35
Babusiaux C. et al., 2010, A&A, 519, A77
Bender R., 1990, A&A, 229, 441
Bettoni D., Galletta G., 1994, A&A, 281, 1
Bournaud F., Elmegreen B. G., Elmegreen D. M., 2007, ApJ, 670, 237
Bureau M., Athanassoula E., 2005, ApJ, 626, 159
Bureau M., Freeman K. C., 1999, AJ, 118, 126
Bureau M., Aronica G., Athanassoula E., Dettmar R.-J., Bosma A., Freeman K. C., 2006, MNRAS, 370, 753
Burstein D., Faber S. M., Gaskell C. M., Krumm N., 1984, ApJ, 287, 586
Cappellari M., Emsellem E., 2004, PASP, 116, 138
Carlberg R. G., 1984, ApJ, 286, 403
Carollo C. M., Scarlata C., Stiavelli M., Wyse R. F. G., Mayer L., 2007, ApJ, 658, 960
Chung A., Bureau M., 2004, AJ, 127, 3192
Cole S., Aragon-Salamanca A., Frenk C. S., Navarro J. F., Zepf S. E., 1994, MNRAS, 271, 781
Combes F., Debbasch F., Friedli D., Pfenniger D., 1990, A&A, 233, 82
Davies R. L., Efstathiou G., Fall S. M., Illingworth G., Schechter P. L., 1983, ApJ, 266, 41
de Zeeuw P. T. et al., 2002, MNRAS, 329, 513
Dutton A. A., 2009, MNRAS, 396, 121
Edvardsson B., Andersen J., Gustafsson B., Lambert D. L., Nissen P. E., Tomkin J., 1993, A&A, 275, 101
Eggen O. J., Lynden Bell D., Sandage A. R., 1962, ApJ, 136, 748
Elmegreen D. M., Elmegreen B. G., Hirst A. C., 2004, ApJ, 604, L21

Emsellem E. et al., 2004, MNRAS, 352, 721

Eskridge P. B. et al., 2000, AJ, 119, 536

Falcón-Barroso J. et al., 2004, MNRAS, 350, 35

Falcón-Barroso J. et al., 2006, MNRAS, 369, 529

Fisher D., Illingworth G., Franx M., 1994, AJ, 107, 160

Freeman K. C., 2008, in Bureau M., Athanassoula E., Barbuy B., eds, Proc. IAU Symp. 245, Formation and Evolution of Galaxy Bulges. Kluwer, Dordrecht, p. 3

Gadotti D. A., dos Anjos S., 2001, AJ, 122, 1298

Hopkins P. F., Kereš D., Ma C., Quataert E., 2010, MNRAS, 401, 1131

Howard C. D. et al., 2009, ApJ, 702, L153

Jarvis B., 1990, in Wielen R., ed., Dynamics and Interactions of Galaxies. Springer, Berlin, p. 416

Kormendy J., Illingworth G., 1982, ApJ, 256, 460

Kormendy J., Kennicutt R. C., Jr, 2004, ARA&A, 42, 603

Kormendy J., Drory N., Bender R., Cornell M. E., 2010, ApJ, 723, 54

Kuijken K., Merrifield M. R., 1995, ApJ, 443, L13

Kuntschner H., 2000, MNRAS, 315, 184

Kuntschner H. et al., 2006, MNRAS, 369, 497

Kuntschner H. et al., 2010, MNRAS, 408, 97

Larson R. B., 1974, MNRAS, 166, 585

Lütticke R., Dettmar R.-J., Pohlen M., 2000, A&AS, 145, 405

MacArthur L. A., González J. J., Courteau S., 2009, MNRAS, 395, 28

Marinova I., Jogee S., 2007, ApJ, 659, 1176

Méndez-Abreu J., Corsini E. M., Debattista V. P., De Rijcke S., Aguerri J. A. L., Pizzella A., 2008, ApJ, 679, L73

Merrifield M. R., Kuijken K., 1999, A&A, 345, L47

Noguchi M., 1999, ApJ, 514, 77

Norris M. A., Sharples R. M., Kuntschner H., 2006, MNRAS, 367, 815

Paudel S., Lisker T., Kuntschner H., Grebel E. K., Glatt K., 2010, MNRAS, 405, 800

Peletier R. F., Balcells M., Davies R. L., Andredakis Y., Vazdekis A., Burkert A., Prada F., 1999, MNRAS, 310, 703

Pipino A., Matteucci F., 2004, MNRAS, 347, 968

Proctor R. N., Sansom A. E., 2002, MNRAS, 333, 517

Proctor R. N., Sansom A. E., Reid I. N., 2000, MNRAS, 311, 37

Prugniel P., Soubiran C., 2001, A&A, 369, 1048

Raha N., Sellwood J. A., James R. A., Kahn F. D., 1991, Nat, 352, 411

Sánchez-Blázquez P. et al., 2006, MNRAS, 371, 703

Sarzi M. et al., 2006, MNRAS, 366, 1151

Sellwood J. A., Wilkinson A., 1993, Rep. Progress Phys., 56, 173

Shaw M., 1993, A&A, 280, 33

Shaw M., Wilkinson A., Carter D., 1993, A&A, 268, 511

Shen J., Rich R. M., Kormendy J., Howard C. D., De Propris R., Kunder A., 2010, ApJ, 720, L72

Thomas D., Davies R. L., 2006, MNRAS, 366, 510

Thomas D., Greggio L., Bender R., 1999, MNRAS, 302, 537

Thomas D., Maraston C., Bender R., 2003, MNRAS, 339, 897

Trager S. C., Worthey G., Faber S. M., Burstein D., Gonzalez J. J., 1998, ApJS, 116, 1

van den Bosch F. C., 2001, MNRAS, 327, 1334

White S. D. M., Rees M. J., 1978, MNRAS, 183, 341

Whyte L. F., Abraham R. G., Merrifield M. R., Eskridge P. B., Frogel J. A., Pogge R. W., 2002, MNRAS, 336, 1281

Worthey G., 1994, ApJS, 95, 107

Zoccali M., Hill V., Lecureur A., Barbuy B., Renzini A., Minniti D., Gómez A., Ortolani S., 2008, A&A, 486, 177

This paper has been typeset from a TeX/LaTeX file prepared by the author.